ResearchGate

See discussions, stats, and author profiles for this publication at: https://www.researchgate.net/publication/260130853

The changing point-spread function: Single-molecule-based super-resolution imaging

ARTICLE *in* HISTOCHEMIE · FEBRUARY 2014

Impact Factor: 3.05 · DOI: 10.1007/s00418-014-1186-1 · Source: PubMed

CITATIONS
6

READS
65

4 AUTHORS, INCLUDING:

Mathew Horrocks
University of Cambridge
19 PUBLICATIONS **74** CITATIONS
SEE PROFILE

Steven F. Lee
University of Cambridge
31 PUBLICATIONS **493** CITATIONS
SEE PROFILE

All in-text references underlined in blue are linked to publications on ResearchGate, letting you access and read them immediately.

Available from: Mathew Horrocks
Retrieved on: 27 January 2016

Histochem Cell Biol (2014) 141:577–585
DOI 10.1007/s00418-014-1186-1

REVIEW

The changing point-spread function: single-molecule-based super-resolution imaging

Mathew H. Horrocks · Matthieu Palayret · David Klenerman · Steven F. Lee

Accepted: 20 January 2014 / Published online: 11 February 2014
© Springer-Verlag Berlin Heidelberg 2014

Abstract Over the past decade, many techniques for imaging systems at a resolution greater than the diffraction limit have been developed. These methods have allowed systems previously inaccessible to fluorescence microscopy to be studied and biological problems to be solved in the condensed phase. This brief review explains the basic principles of super-resolution imaging in both two and three dimensions, summarizes recent developments, and gives examples of how these techniques have been used to study complex biological systems.

Keywords Single-molecule microscopy · Super-resolution imaging · PALM/(d)STORM imaging · Localization microscopy

Fluorescence microscopy allows users to dynamically observe phenomena in living cells; however, the wave nature of light and its associated diffraction restrict the resolution of light microscopy: When light of wavelength λ is focused by a lens with a numerical aperture NA, objects that are closer together than $d = \lambda/(2\mathrm{NA})$ cannot be easily discerned. This is the Abbe diffraction limit (Abbe 1873), and it has until recently restricted the resolution of fluorescence microscopy to ~250 nm. New methods, collectively grouped under the term super-resolution (SR) microscopy, have been developed to overcome this physical limit, gaining over two orders of magnitude in precision (Szymborska et al. 2013), allowing direct observation of processes at spatial scales much more compatible with the regime that biomolecular interactions take place on. Radically, different approaches have so far been proposed, including limiting the illumination of the sample to regions smaller than the diffraction limit (targeted switching and readout) or stochastically separating single fluorophores in time to gain resolution in space (stochastic switching and readout). The latter also described as follows: Single-molecule active control microscopy (SMACM), or single-molecule localization microscopy (SMLM), allows imaging of single molecules which cannot only be precisely localized, but also followed through time and quantified. This brief review will focus on this "pointillism-based" SR imaging and its application to biological imaging in both two and three dimensions.

When observed through any optical imaging system, a single-point emitter is blurred due to the diffractive properties of light. This blur, or point-spread function (PSF), of the point emitter is not due to an imperfect focus of the optics, but is an inherent property of the wave-like nature of light. The PSF can be well approximated by a 2D-Gaussian function, the width of which is proportional to the emitted wavelength (Santos and Young 2000). The PSF can be thought of as a probability distribution function of the position of the point emitter; therefore, through determination of the center of an individual PSF, the Abbe diffraction limit can be overcome and the emitter can be localized at SR. The calculation of the PSF center and consequently the precision of the localization are dependent on two main properties: the number of photons detected N, via $1/\sqrt{N}$, and the pixel size of the camera (Thompson et al. 2002).

The essential step leading to pointillism-based SR microscopy was the ability to control the activation of point

Mathew H. Horrocks and Matthieu Palayret have contributed equally.

M. H. Horrocks · M. Palayret · D. Klenerman · S. F. Lee (✉)
Department of Chemistry, University of Cambridge, Lensfield Road, Cambridge CB2 1EW, UK
e-mail: sl591@cam.ac.uk

emitters, and the techniques now distinguish themselves based on how emitters are spatially isolated. The first pointillism-based SR techniques were all demonstrated in 2006, and these were photo-activated localization microscopy (PALM) (Betzig et al. 2006), stochastic optical reconstruction microscopy (STORM) (Rust et al. 2006), and fluorescence photo-activation localization microscopy (fPALM) (Hess et al. 2006).

One requirement for accurate super-localization is that the point emitters are well separated in space so that their PSFs do not overlap. This is rarely possible with biological structures, meaning that innovative methods for decreasing the concentration of active fluorophores and separating dense or agglomerated emitters have had to be developed. Generally, this involves stochastically switching a subset of fluorophores on at any given time, imaging them, determining their PSF centers, and then switching them off. This process is then repeated with other emitters, and multiple cycles allow a SR image to be built up from the fitted centers (Fig. 1b). This requires methods for switching fluorophores "on" and "off," and many solutions to this exist. In this review, we highlight three popular classes used in biological imaging: exploiting the innate photo-physics of fluorophores, chemical/spectral structural modification, and finally diffusion.

Photo-physical manipulation

When pumped to their excited states, organic dyes can relax via a number of mechanisms (Fig. 1a). Fluorescence occurs when the fluorophore relaxes from its first excited singlet state (S_1) via emission of a photon, with a temporal probability well modeled by an exponential decay and characteristic fluorescence lifetime (τ) on the order of nanoseconds. However, inter-system crossing to non-fluorescent states, such as triplet states (T_n), may also occur, and when in such states, the fluorophores are unable to rapidly relax and enter further excitation-emission cycles, here the fluorescence lifetime is typically on the order of micro- to milliseconds. This leads to the molecules undergoing fluorescence

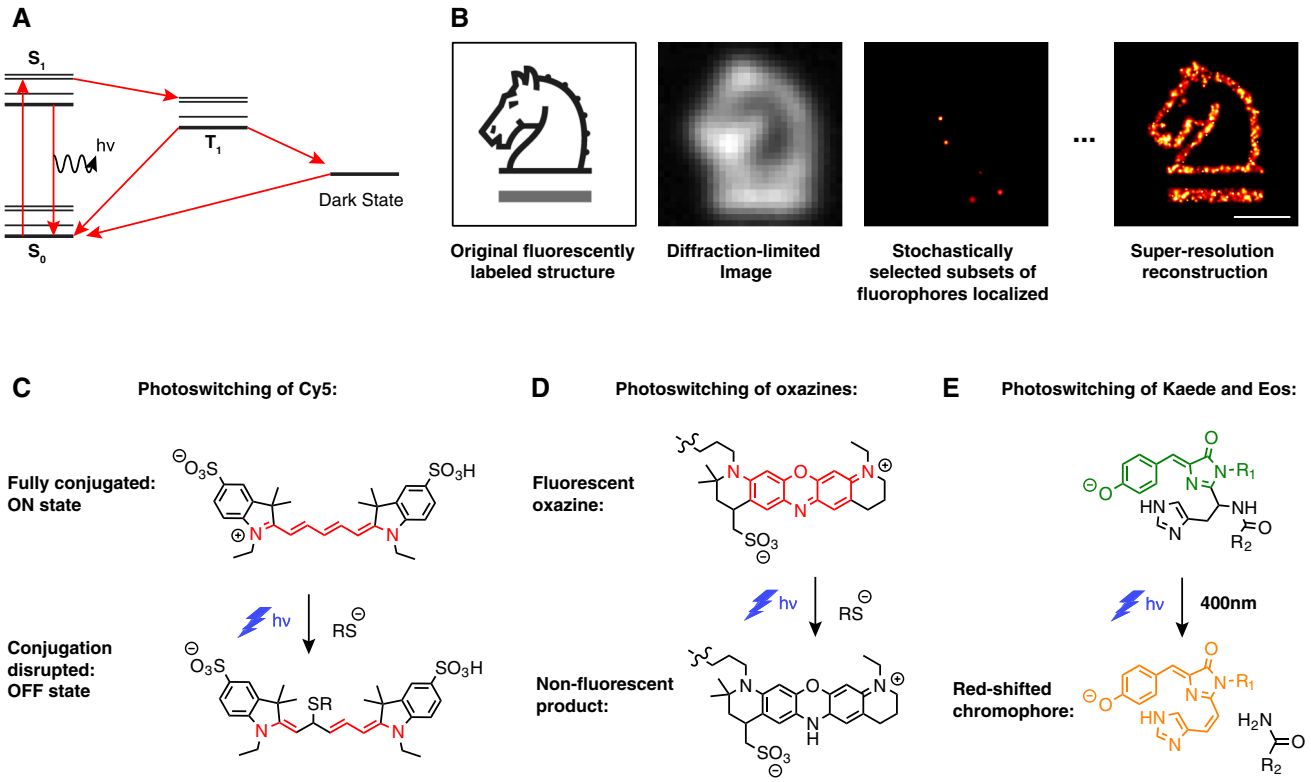

Fig. 1 Photo-physics of organic fluorophores and basis for SR imaging. **a** Modified Jablonski diagram including intersystem crossing to the first triplet state, and transition to a generic dark state. **b** Principles of stochastic SR. From the *left*, the "Springer Horse" (2.2 μm × 2.2 μm) is simulated labeled with fluorophores. In the next image, simulated data of all of the dye molecules emitting simultaneously, and so the diffraction-limited images overlap on the camera, and information about the underlying structure cannot be resolved. In the next image, on–off control of the fluorophore between "on" and "off" states allows individual fluorophores to be localized. Repetition of this procedure gives the final SR image (*right*). *Scale bar* is 1 μm in length. **c** Photo-switching of Cy5 by formation of a thiol adduct. **d** Photo-chemical reduction in the oxazine ATTO655 chromophore. **e** Photo-chemical switching of the chromophore in the fluorescent proteins Eos and Kaede

intermittently, so-called blinking, as they cycle into and out of the "dark" state. Unfortunately, population of these dark states can often be part of the photo-bleaching pathway, and so the number of switching cycles is limited. However, this blinking can still be used to temporally separate the emitters and therefore allow for SR imaging (Hell and Kroug 1995). This process is also observed in genetically encodable fluorescent proteins (FPs), for example enhanced yellow fluorescent protein (eYFP), which has been shown to undergo power-dependent blinking under irradiation of 514-nm laser excitation; this has been used to study super-resolved spatial distributions of proteins in bacterial models (Ptacin et al. 2010; Lee et al. 2011).

An alternative strategy to control the photo-physics of fluorophores is to perturb the excited state kinetics. For instance, the fluorescence quantum yield of far-red fluorophores is typically low; however, non-radiative decay routes can be selectively turned off through the use of deuterated (heavy) water-based buffers, leading to an increase in the fluorescence quantum yield by, in some cases, over 200 %. This has been shown in multiple common classes of dyes, including oxazines and cyanines (Lee et al. 2013; Klehs et al. 2013).

Chemical modification

To circumvent the effect of photo-bleaching, various methods have been employed to remove molecular oxygen from solution, for example by simple degassing or through addition of enzymatic oxygen scavenger systems (Englander et al. 1987; Aitken et al. 2008; Swoboda et al. 2012). However, the removal of molecular oxygen leads to the triplet-state lifetime increasing, and so blinking becomes more noticeable. The addition of triplet-state quenchers or reducing agents, such as Trolox (Rasnik et al. 2006) and β-mercaptoethanol (Harada et al. 1990), leads to the suppression of this blinking, as they are able to relax the dye back to the ground state. In addition to adding only reducing agents, a refined system that also uses oxidizing agents has been developed in what is referred to as a reducing and oxidizing system (ROXS) (Vogelsang et al. 2008). In such a system, micro- to millimolar concentrations of reducing and oxidizing agents are added to the oxygen-depleted buffer. These then quench the fluorophores occupying the triplet state, by either reduction or oxidation to the corresponding semi-reduced anion or semi-oxidized cation. The anion or cation is then either oxidized or reduced again, respectively, yielding the singlet ground state.

By varying the buffer composition (i.e., the concentrations of the oxidizing and reducing agents), long-lasting off-states corresponding to the semi-reduced or semi-oxidized ions can be generated, therefore allowing for SR imaging. In STORM, Cyanine 5 (Cy5) is excited with red laser light in oxygen-depleted buffers containing a thiol (Heilemann et al. 2005), and it can enter a meta-stable dark state, caused via thiol addition to the excited state of the fluorophore (Dempsey et al. 2009) (Fig. 1c). This dark state can be depopulated through irradiation with a shorter wavelength of light yielding the on-state of the dye once again. Excitation at this shorter wavelength can either be achieved directly (van de Linde et al. 2011b), or by using a reporter–activator dye pair(Dempsey et al. 2011), for example Cy5–Cy3, where the close proximity of the two dyes leads to the on-switching of the reporter, Cy5, at lower laser powers. This photo-switching has also been successfully implemented with other cyanine dyes, such as Alexa Fluor 647 (Heilemann et al. 2005), Cy5.5 (Heilemann et al. 2008), Cy7 (Bates et al. 2007), Alexa Fluor 680 (van de Linde et al. 2011b), Alexa Fluor 700 (Baddeley et al. 2011), and Alexa Fluor 750 (Lampe et al. 2012). Rhodamines and oxazines (Fig. 1d) can also be switched using various buffer conditions, for example, switching occurs in the presence of thiols (millimolar concentrations) (Heilemann et al. 2009; van de Linde et al. 2011a; Dempsey et al. 2011) with tris(2-carboxyethyl)phosphine (TCEP) (Vaughan et al. 2013) and reducing/oxidizing agents (Steinhauer et al. 2008; Heilemann et al. 2009; Vogelsang et al. 2009). The dark state exists as a reduced form of the chromophore, which is able to absorb at shorter wavelengths, enabling it to be re-activated with 350–550-nm radiation. It is also possible to form hydrogenated fluorophores which act as dark states, for example standard fluorophores such as Cy3, Cy3B, Alexa Fluor 647, Cy5.5, and ATTO 488 can be reduced with sodium (Kundu et al. 2009), and upon excitation with 405-nm radiation, the fluorescent form of the dye is recovered allowing for SR localization.

Diffusion

In addition to photo-switchable fluorophores, techniques that rely on fluorophores being transiently bound to the biomolecule of interest have been developed. In point accumulation for imaging in nanoscale topography (PAINT) (Sharonov and Hochstrasser 2006) and uniform PAINT (uPAINT) (Giannone et al. 2010), fluorescent molecules temporarily bind to surfaces, such as membranes, and are localized allowing for SR imaging. Binding-activated localization microscopy (BALM) (Schoen et al. 2011) has been used to generate SR images of DNA, using the intercalating dye YOYO-1, the quantum yield of which increases threefold on binding to DNA.

Fluorescent proteins for SR imaging

Light-inducible control of the spectroscopic properties of FPs allows them to be both used to generate SR images

and targeted with genetic specificity. There are many different FPs; however, they all consist of a single polypeptide chain of about 230 amino acids in length, each containing an 11-stranded β-barrel, which has a single distorted helix spiraling down its center and contains three amino acids that form the chromophore (Dedecker et al. 2013). The chromophore engages in a wide range of interactions with surrounding amino acids and solvent environments, and single mutations in the non-chromophore amino acids can strongly influence the spectroscopic properties of the protein, shifting its absorption and emission spectrum, or even leading to it becoming non-fluorescent (Tsien 1998). There are a number of different classes of FPs that can be used in SR microscopy. The first type displays a light-induced, reversible transition between a fluorescent and non-fluorescent state and occurs in a wide range of FPs (Dickson et al. 1997; Jung et al. 2001a, b; Chudakov et al. 2003; Shaner et al. 2008), some of which give rise to very high contrast, good thermal reversibility and high thermal stability, examples including Dronpa (Ando et al. 2004), mTFP0.7 (Henderson et al. 2007), rsTagRFP (Subach et al. 2010), rsEGFP (Grotjohann et al. 2011), and mGeos (Chang et al. 2012). This type of photoswitching usually involves a transition to the off-state after irradiation with the same wavelength that induces fluorescent emission, while irradiation with UV light leads to recovery of the on-state. The second class of FPs are those that display irreversible light-induced changes, either consisting of an off-state to on-state conversion, or those that convert from shorter to longer wavelength emission (green to red), when irradiated with blue/UV light. Examples of the first type include PA-GFP (Patterson and Lippincott-Schwartz 2002), PS-CFP (Chudakov et al. 2004), and PAmCherry (Subach et al. 2009). Examples of those that undergo color conversion include Kaede (Ando et al. 2002), EosFP (Wiedenmann et al. 2004), and its monomeric/tandem variants, Dendra2 (Gurskaya et al. 2006), mKikGR (Habuchi et al. 2008), and PSmOrange (Subach et al. 2011, 2012). The green to red photo-conversion is a result of the conjugated system in the chromophore being extended due to cleavage of a histidine side chain (Mizuno et al. 2003; Nienhaus et al. 2005) (Fig. 1e). The major advantage of this type of FP is that structures are able to be observed before photo-conversion, the fluorescence can then be switched on, and individual proteins localized before they are photo-bleached. mEos has proved popular for PALM imaging due to facile conversion into the longer wavelength bright form; however, its complex photo-physics are yet to be fully understood, limiting its use in stoichiometric studies. Furthermore, its spectral position within the visible spectrum limits its use in two-color imaging. One issue with performing such experiments has been the over-counting of single molecules due to blinking (Annibale et al. 2011) and the under-counting due to misfolding or incomplete activation of FPs (Durisic et al. 2014); however, new analytical methods have been developed taking these issues into account, allowing for more precise quantification in quantitative PALM experiments (Sengupta et al. 2011; Lee et al. 2012).

Biological insights with 2D SR microscopy

Over the past 8 years, SR techniques have been extensively used to image cellular structures. Traditionally, cytoskeletal networks have been used to test new methods, as they have a well-characterized linear structure with widths below the diffraction limit. The scope of these SR measurements has increased substantially and successfully applied to study many more varied systems. One example being the imaging of bacterial cells (where the physical dimensions of the organism approach the spatial regime of the diffraction limit) to study the organization and spatial distribution of regulatory proteins, such as HU (Lee et al. 2011) and ParA (Ptacin and Shapiro 2013) in *Caulobacter crescentus* (Fig. 2a). This imaging approach has allowed not only higher contrast, and greater resolution to be achieved, but also to obtain quantitative information such as the distribution and clustering behavior of such proteins (Lillemeier et al. 2010). Interesting sub-cellular protein complexes have also been super-resolved: Doksani et al. (2013) imaged the t-loop sub-structure of telomeres by SR-FISH (Fig. 2b).

Recently, optical imaging at sub-nanometer resolution has been achieved, bridging the gap between structural biology and SR microscopy. By averaging many images of single nuclear pore complexes, Szymborska et al. (2013) have successfully localized the radial positions of its different units with a precision of 0.2 nm, in vivo (Fig. 2c). Superposing their results with the EM structure of the rigid nuclear pore complex has allowed them to directly visualize and confirm specific structural models.

3D SR microscopy

Although biological processes occur in three dimensions, most imaging techniques measure a 2D projection of a 3D volume. Separating single proteins in the axial dimension is necessary to avoid inaccurate densities and allow for dynamic analyses and quantification. Although total internal reflection microscopy (TIRFM) has been extensively used to investigate many biological processes happening at the basal 2D cell membrane (Dunne et al. 2009; Narayan et al. 2013), many intracellular processes have largely been left unexplored.

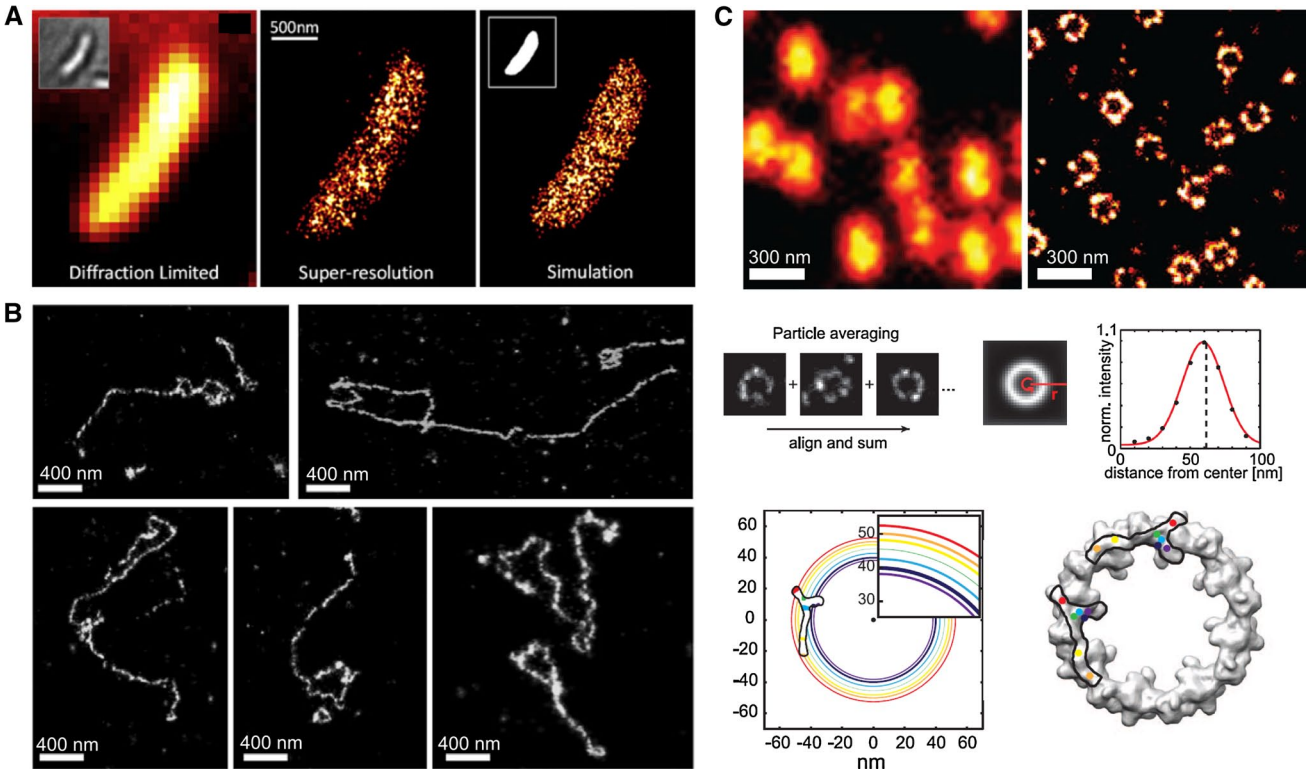

Fig. 2 SR microscopy was applied to resolve 2D biological structures. **a** HU2-eYFP was imaged in fixed *C. crescentus* with a 514-nm laser. The SR reconstruction (*middle panel*) brings quantitative information about the distribution of the protein, which diffraction-limited image does not give (*left panel*—white light transmission image in the *inset*). Comparison of the protein distribution with a Monte Carlo simulation of a random distribution of molecules inside the model cell volume (*right panel*—projection of the model cell volume in the *inset*) shows that the protein is significantly clustered. [Figure 1b–d from (Lee et al. 2011)]. **b** Telomeres from mouse splenocytes were hybridized with Alexa 647-labelled FISH probes and imaged in a relaxed configuration after cyto-centrifugation. Individual super-resolved telomeres present a T-loop structure. [Figure 1d from (Doksani et al. 2013)]. **c** The nucleopore complexes of U2OS cell nuclei were labeled with an anti-Nup133 Alexa 647-labelled antibody and imaged by confocal (*top row, left*) or SR (*top row, right*) microscopy. Single labeled pores were aligned (*middle row, left*) and summed (*middle row, center*) in order to precisely super-localize the average distance of the fluorophore from the center of the structure (*middle row, right*) with a sub-nanometer precision. The experiment was repeated for several proteins of the pore complex (different colors in the *bottom row, left panel*). The different radial distances allowed to exclude some incompatible models of the arrangements of the pore complex and to confirm the compatibility of others (example of a compatible model in the *bottom row, right panel*). [Figure 1a–e, 4a, c from (Szymborska et al. 2013)]

Different methods have been developed to gain SR information about the axial positions of biomolecules. These are either based on the axial form of the PSF, or on interferometry. However, the gain in information from the third dimension is obtained to the detriment of both precision (due to effects such as the addition of extra optical components to the imaging system, the dilation of the PSF over more pixels and the increase in out-of-focus noise) and resolution (due to the need of increased sampling when gaining another dimension) (Lakadamyali et al. 2012).

It is the way in which the PSFs change in space that axially encodes positional information. Here we describe four 3D SR techniques (summarized in Fig. 3a) that have different advantages and disadvantages and can be compared using different criteria: complexity, commercial availability, axial precision (Rieger and Stallinga 2013), and uniformity of the axial precision. A way to compare the efficiency of the 3D PSFs to encode lateral and axial positions is to look at their Fisher information, which allows calculating their theoretical localization precisions for different signal-to-noise situations (Fig. 3b) (Badieirostami et al. 2010).

In biplane SR microscopy (Juette et al. 2008), each fluorophore is simultaneously imaged at two different (axial) z-planes. The difference in their recorded PSFs at each of the two planes allows one to obtain its axial position with an accuracy of typically 75 nm. This method is relatively easy to implement and commercially available, but has a systematic non-uniformity of the axial precision, dependant on where in space (relative to the focal plane) the localization originated from (Fig. 3b). Moreover, since it requires

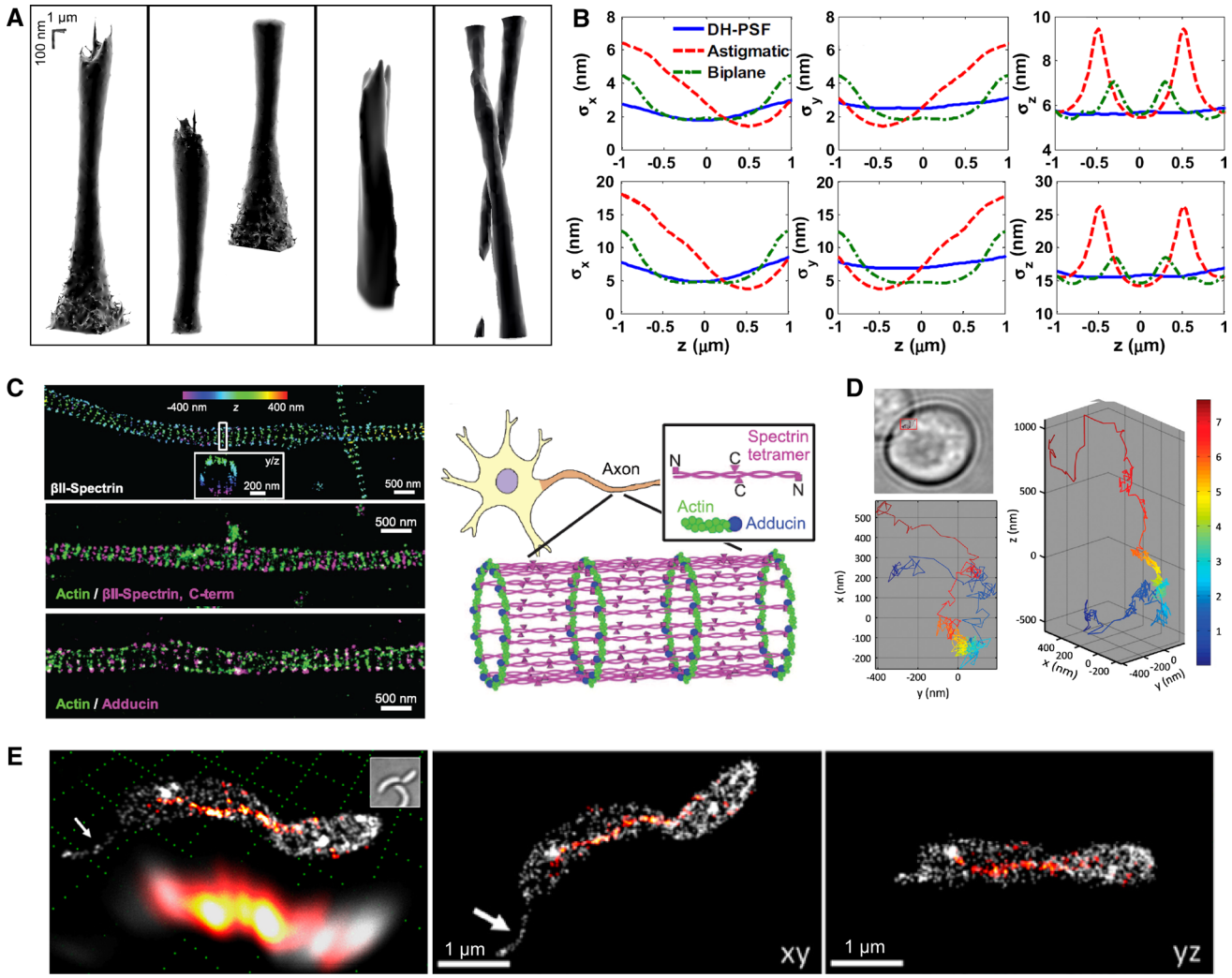

Fig. 3 Different 3D PSFs are used in SR microscopy to resolve 3D biological structures. **a** Diffraction-limited beads were immobilized onto a coverslip and imaged at different *z*-planes (every 20 nm) from 1 µm below the focal plane to 1 µm above it. Individual PSFs were summed, and their 3D shapes were rendered (from *left* to *right*: usual PSF, bi-plane PSFs, astigmatism PSF, and DH-PSF). *Scale bars* 1 µm in *x* and *y*, 100 nm in *z*. [Palayret and Lee (unpublished data)]. **b** The theoretical Fisher information for lateral (*left* and *middle columns*) and axial (*left column*) precisions for all 3D PSFs varies in *z*. The amplitude of the precisions depends on the signal-to-background ratio (*top* 6,000 photons, *bottom* 1,000 photons detected on the CCD with two photons/pixel background level in each case), but not their shapes. The DH-PSF, however, has more uniform localization precision than the other two methods in all three dimensions. [Figure 2 from (Badieirostami et al. 2010)]. **c** Spectrin, actin, and adducing were imaged in fixed and immuno-labeled axons with 3D astigmatism STORM. The distribution of spectrin is strikingly organized in very regularly spaced rings along the axon (*left column, top panel*). Two-color SR experiments (l*eft column*, *middle*, and *bottom panels*) reveal a coordinated, quasi-1D-lattice structure of actin and adducing in between the rings of spectrin, leading to a refined structural model for the cortical cytoskeleton in axons. [Figure 4 from (Xu et al. 2013)]. **d** Single mRNA-protein complexes were super-localized and tracked in three dimensions using the DH-PSF in live budding yeast (white light transmission image of the yeast cell in *top-left panel*). The comparison between the 2D (*bottom left*) and 3D (*right panel*) trajectories of the same complex underlines how important the third dimension is to observe unbiased phenomena: The apparent directed motion in *z* is not apparent in the 2D projection of the trajectory. [Figure 1 from (Thompson et al. 2010)]. **e** Crescentin tagged with eYFP was imaged in live *C. crescentus* cells using 3D DH-PSF SR microscopy. The cell membrane was consecutively imaged in 3D SR to obtain the contour of the cell. The *left panel* shows a 3D SR (*top*) and diffraction-limited (*bottom*) perspective images of a predivisional cell (the crescentin fiber is colored in *red* inside the cell membrane represented in *gray*). A white light transmission image is given in the *inset*. A 2D isometric *xy* (*middle*) and *yz* (*right panel*) projections are also shown. The stalk of the cell is indicated by the *arrows*. *Grid and scale bars* 1 µm. [Figure 2d–f from (Lew et al. 2011b)]

imaging the emitted signal twice, the signal is intrinsically divided by two and twice as many pixels are needed, somewhat limiting the field of view.

Astigmatism SR microscopy adds a cylindrical lens in the imaging path in order to create an asymmetry above and below the focal plane, allowing the axial position of

the fluorophore to be coded in the ratio of both x and y widths of the detected 2D PSF (Huang et al. 2008). This method is relatively easy to implement and is commercially available. However, a fast moving fluorophore in the focal plane in a live cell would be imaged as a blurred elliptic PSF (Deschout et al. 2012; Rowland and Biteen 2013) and could consequently be axially mislocalized. Also, the axial localization precision, though more uniform than for biplane microscopy (typically of ~20 nm), still varies along the axial plane (Fig. 3b).

One way to avoid the non-uniformity of the axial localization precision is to modify or even engineer the 3D-PSF so that the change of the PSF in z is fundamentally independent of where the localization originated (Fig. 3b). The Moerner group has pioneered the use of a number of different PSFs in SR imaging, obtaining more uniform localization precision in the 3D. The concept behind the double-helix (DH) (Pavani et al. 2009), or the corkscrew (Lew et al. 2011a) PSFs, is to modify the phase of the emitted signal in a 4-f optical system (by use of a phase plate or a spatial light modulator) in order to encode the z-position of the emitter in an angle. The DH-PSF method divides the initial PSF into two (or one in the case of the corkscrew PSF) spots rotating about a z-axis as a function of their z-position (Fig. 3a). These methods are slightly more complex to implement and are still not commercially available. However, the range for a full rotation of the PSF can be tuned and optimized for the depth of the structure of interest. Axial resolutions of ~30 nm are typically achieved (similar than for astigmatism) across the whole depth of field (~2 μm) (Lew et al. 2011b).

The last and most precise method is interferometric PALM (iPALM) (Shtengel et al. 2009). Light emitted is collected by two focused objective lenses and is then interfered through two dichroic mirrors and projected onto multiple CCD cameras. The axial position of the emitter is determined by the specific intensity ratios of the three PSFs simultaneously recorded on the cameras. This method presents a strict uniform axial localization precision (~5 nm). However, because of the dual objective required for the division of the signal onto three different cameras, samples thicker than twice the working distance of the objectives cannot be observed. Moreover, such a method is technically demanding to implement, and more susceptible to instabilities of the instrumentation when compared to the other methods and is not currently commercially available.

3D SR microscopy in biology

These recent developments in 3D methods have led to many more structures being studied in 3D. As in 2D SR microscopy, cytoskeletal structures are useful for validating methods and precision. Olivier et al. (2013) used biplane microscopy, together with astigmatism for greater precision, to image tubulin in fixed cells. The cytoskeletal structure of axons has been further refined by Xu et al. (2013). Using astigmatism, they discovered very periodic actin and spectrin rings spanning neuronal axons, separated by 190 nm (Fig. 3c). This exciting discovery could not have been resolved without SR imaging: The characteristic ring structures and the inter-ring separation are both smaller than the diffraction limit (250 nm).

Cytoskeletal protein super-structures were also imaged in live *Caulobacter crescentus* cells using the DH-PSF. Crescentin and the cell membrane were sequentially imaged, demonstrating the ability to super-resolve 3D structures in live bacterial cells (Fig. 3e) (Lew et al. 2011b). In addition to structural information, super-resolved 3D tracking of biomolecules can be performed. Thompson et al. (Lee et al. 2011) tagged single mRNAs in live budding yeast and studied their dynamic properties. Localization of the trajectory in the third dimension is essential: This is highlighted with examples of 2D (ostensibly fixed) mRNA, which are in reality moving extensively in z (Fig. 3d).

Conclusion

Research into cell biology is going through an important change. Monitoring molecular phenomena in cells at precisely defined locations, as opposed to the entire cell, bulk tissue or in vitro methods has become essential for understanding the mechanisms under study. SR techniques are beginning to allow us to see inside cells, allowing molecular scale events to be visualized as never before, as they unfold. It is expected that future work into areas such as instrument development (including stability, optical aberration correction, and dipole orientation effects) and rational fluorophore design (improving the brightness and stability of dyes, and switching mechanisms) will enable us to reach a new frontier to observe new super-resolved structures which will answer major questions in biomedical imaging.

References

Abbe E (1873) Beiträge zur theorie des mikroskops und der mikroskopischen wahrnehmung. Arch F Microsc Anat 9:413–468

Aitken CE, Marshall RA, Puglisi JD (2008) An oxygen scavenging system for improvement of dye stability in single-molecule fluorescence experiments. Biophys J 94:1826–1835. doi:10.1529/biophysj.107.117689

Ando R, Hama H, Yamamoto-Hino M et al (2002) An optical marker based on the UV-induced green-to-red photoconversion of a fluorescent protein. Proc Natl Acad Sci USA 99:12651–12656. doi:10.1073/pnas.202320599

Ando R, Mizuno H, Miyawaki A (2004) Regulated fast nucleocytoplasmic shuttling observed by reversible protein highlighting. Science 306:1370–1373. doi:10.1126/science.1102506

Annibale P, Vanni S, Scarselli M et al (2011) Quantitative photo activated localization microscopy: unraveling the effects of photoblinking. PLoS ONE 6:e22678. doi:10.1371/journal.pone.0022678

Baddeley D, Crossman D, Rossberger S et al (2011) 4D super-resolution microscopy with conventional fluorophores and single wavelength excitation in optically thick cells and tissues. PLoS ONE 6:e20645. doi:10.1371/journal.pone.0020645

Badieirostami M, Lew MD, Thompson MA, Moerner WE (2010) Three-dimensional localization precision of the double-helix point spread function versus astigmatism and biplane. Appl Phys Lett 97:161103. doi:10.1063/1.3499652

Bates M, Huang B, Dempsey GT, Zhuang X (2007) Multicolor super-resolution imaging with photo-switchable fluorescent probes. Science 317:1749–1753. doi:10.1126/science.1146598

Betzig E, Patterson GH, Sougrat R et al (2006) Imaging intracellular fluorescent proteins at nanometer resolution. Science 313:1642–1645. doi:10.1126/science.1127344

Chang H, Zhang M, Ji W et al (2012) A unique series of reversibly switchable fluorescent proteins with beneficial properties for various applications. Proc Natl Acad Sci USA 109:4455–4460. doi:10.1073/pnas.1113770109

Chudakov DM, Belousov VV, Zaraisky AG et al (2003) Kindling fluorescent proteins for precise in vivo photolabeling. Nat Biotechnol 21:191–194. doi:10.1038/nbt778

Chudakov DM, Verkhusha VV, Staroverov DB et al (2004) Photoswitchable cyan fluorescent protein for protein tracking. Nat Biotechnol 22:1435–1439. doi:10.1038/nbt1025

Dedecker P, De Schryver FC, Hofkens J (2013) Fluorescent proteins: shine on, you crazy diamond. J Am Chem Soc 135:2387–2402. doi:10.1021/ja309768d

Dempsey GT, Bates M, Kowtoniuk WE et al (2009) Photoswitching mechanism of cyanine dyes. J Am Chem Soc 131:18192–18193. doi:10.1021/ja904588g

Dempsey GT, Vaughan JC, Chen KH et al (2011) Evaluation of fluorophores for optimal performance in localization-based super-resolution imaging. Nat Methods 8:1027–1036. doi:10.1038/nmeth.1768

Deschout H, Neyts K, Braeckmans K (2012) The influence of movement on the localization precision of sub-resolution particles in fluorescence microscopy. J Biophotonics 5:97–109. doi:10.1002/jbio.201100078

Dickson RM, Cubitt AB, Tsien RY, Moerner WE (1997) On/off blinking and switching behaviour of single molecules of green fluorescent protein. Nature 388:355–358. doi:10.1038/41048

Doksani Y, Wu JY, de Lange T, Zhuang X (2013) Super-resolution fluorescence imaging of telomeres reveals TRF2-dependent T-loop formation. Cell 155:345–356. doi:10.1016/j.cell.2013.09.048

Dunne PD, Fernandes RA, McColl J et al (2009) DySCo: quantitating associations of membrane proteins using two-color single-molecule tracking. Biophys J 97:L5–L7. doi:10.1016/j.bpj.2009.05.046

Durisic N, Laparra-Cuervo L, Sandoval-Álvarez A et al (2014) Single-molecule evaluation of fluorescent protein photoactivation efficiency using an in vivo nanotemplate. Nat Methods. doi:10.1038/nmeth.2784

Englander SW, Calhoun DB, Englander JJ (1987) Biochemistry without oxygen. Anal Biochem 161:300–306

Giannone G, Hosy E, Levet F et al (2010) Dynamic superresolution imaging of endogenous proteins on living cells at ultra-high density. Biophys J 99:1303–1310. doi:10.1016/j.bpj.2010.06.005

Grotjohann T, Testa I, Leutenegger M et al (2011) Diffraction-unlimited all-optical imaging and writing with a photochromic GFP. Nature 478:204–208. doi:10.1038/nature10497

Gurskaya NG, Verkhusha VV, Shcheglov AS et al (2006) Engineering of a monomeric green-to-red photoactivatable fluorescent protein induced by blue light. Nat Biotechnol 24(4):461–465. doi:10.1038/nbt1191

Habuchi S, Tsutsui H, Kochaniak AB et al (2008) mKikGR, a monomeric photoswitchable fluorescent protein. PLoS ONE 3:e3944. doi:10.1371/journal.pone.0003944

Harada Y, Sakurada K, Aoki T et al (1990) Mechanochemical coupling in actomyosin energy transduction studied by in vitro movement assay. J Mol Biol 216:49–68. doi:10.1016/S0022-2836(05)80060-9

Heilemann M, Margeat E, Kasper R et al (2005) Carbocyanine dyes as efficient reversible single-molecule optical switch. J Am Chem Soc 127:3801–3806. doi:10.1021/ja044686x

Heilemann M, van de Linde S, Schüttpelz M et al (2008) Subdiffraction-resolution fluorescence imaging with conventional fluorescent probes. Angew Chem Int Ed Engl 47:6172–6176. doi:10.1002/anie.200802376

Heilemann M, van de Linde S, Mukherjee A, Sauer M (2009) Super-resolution imaging with small organic fluorophores. Angew Chem Int Ed Engl 48:6903–6908. doi:10.1002/anie.200902073

Hell SW, Kroug M (1995) Ground-state-depletion fluorescence microscopy: a concept for breaking the diffraction resolution limit. Appl Phys B 60:495–497. doi:10.1007/BF01081333

Henderson JN, Ai H-W, Campbell RE, Remington SJ (2007) Structural basis for reversible photobleaching of a green fluorescent protein homologue. Proc Natl Acad Sci USA 104:6672–6677. doi:10.1073/pnas.0700059104

Hess ST, Girirajan TPK, Mason MD (2006) Ultra-high resolution imaging by fluorescence photoactivation localization microscopy. Biophys J 91:4258–4272. doi:10.1529/biophysj.106.091116

Huang B, Wang W, Bates M, Zhuang X (2008) Three-dimensional super-resolution imaging by stochastic optical reconstruction microscopy. Science 319:810–813. doi:10.1126/science.1153529

Juette MF, Gould TJ, Lessard MD et al (2008) Three-dimensional sub-100 nm resolution fluorescence microscopy of thick samples. Nat Methods 5:527–529. doi:10.1038/nmeth.1211

Jung G, Bräuchle C, Zumbusch A (2001a) Two-color fluorescence correlation spectroscopy of one chromophore: application to the E222Q mutant of the green fluorescent protein. J Chem Phys 114:3149–3156. doi:10.1063/1.1342014

Jung G, Wiehler J, Steipe B et al (2001b) Single-molecule microscopy of the green fluorescent protein using simultaneous two-color excitation. ChemPhysChem 2:392–396. doi:10.1002/1439-7641(20010618)2:6<392:AID-CPHC392>3.0.CO;2-7

Klehs K, Spahn C, Endesfelder U et al (2013) Increasing the brightness of cyanine fluorophores for single-molecule and superresolution imaging. ChemPhysChem. doi:10.1002/cphc.201300874

Kundu K, Knight SF, Willett N et al (2009) Hydrocyanines: a class of fluorescent sensors that can image reactive oxygen species in cell culture, tissue, and in vivo. Angew Chem Int Ed Engl 48:299–303. doi:10.1002/anie.200804851

Lakadamyali M, Babcock H, Bates M et al (2012) 3D multicolor super-resolution imaging offers improved accuracy in neuron tracing. PLoS ONE 7:e30826. doi:10.1371/journal.pone.0030826

Lampe A, Haucke V, Sigrist SJ et al (2012) Multi-colour direct STORM with red emitting carbocyanines. Biol Cell 104:229–237. doi:10.1111/boc.201100011

Lee SF, Thompson MA, Schwartz MA et al (2011) Super-resolution imaging of the nucleoid-associated protein HU in *Caulobacter crescentus*. Biophys J 100:L31–L33. doi:10.1016/j.bpj.2011.02.022

Lee S-H, Shin JY, Lee A, Bustamante C (2012) Counting single photoactivatable fluorescent molecules by photoactivated localization microscopy (PALM). Proc Natl Acad Sci USA 109:17436–17441. doi:10.1073/pnas.1215175109

Lee SF, Vérolet Q, Fürstenberg A (2013) Improved super-resolution microscopy with oxazine fluorophores in heavy water. Angew Chem Int Ed Engl 52:8948–8951. doi:10.1002/anie.201302341

Lew MD, Lee SF, Badieirostami M, Moerner WE (2011a) Corkscrew point spread function for far-field three-dimensional nanoscale localization of pointlike objects. Opt Lett 36:202–204

Lew MD, Lee SF, Ptacin JL et al (2011b) Three-dimensional super-resolution colocalization of intracellular protein superstructures and the cell surface in live *Caulobacter crescentus*. Proc Natl Acad Sci USA 108:E1102–E1110. doi:10.1073/pnas.1114444108

Lillemeier BF, Mörtelmaier MA, Forstner MB et al (2010) TCR and Lat are expressed on separate protein islands on T cell membranes and concatenate during activation. Nat Immunol 11:90–96. doi:10.1038/ni.1832

Mizuno H, Mal TK, Tong KI et al (2003) Photo-induced peptide cleavage in the green-to-red conversion of a fluorescent protein. Mol Cell 12:1051–1058

Narayan P, Ganzinger KA, McColl J et al (2013) Single molecule characterization of the interactions between amyloid-β peptides and the membranes of hippocampal cells. J Am Chem Soc 135:1491–1498. doi:10.1021/ja3103567

Nienhaus K, Nienhaus GU, Wiedenmann J, Nar H (2005) Structural basis for photo-induced protein cleavage and green-to-red conversion of fluorescent protein EosFP. Proc Natl Acad Sci USA 102:9156–9159. doi:10.1073/pnas.0501874102

Olivier N, Keller D, Gönczy P, Manley S (2013) Resolution doubling in 3D-STORM imaging through improved buffers. PLoS ONE 8:e69004. doi:10.1371/journal.pone.0069004

Patterson GH, Lippincott-Schwartz J (2002) A photoactivatable GFP for selective photolabeling of proteins and cells. Science 297:1873–1877. doi:10.1126/science.1074952

Pavani SRP, Thompson MA, Biteen JS et al (2009) Three-dimensional, single-molecule fluorescence imaging beyond the diffraction limit by using a double-helix point spread function. Proc Natl Acad Sci USA 106:2995–2999. doi:10.1073/pnas.0900245106

Ptacin JL, Shapiro L (2013) Chromosome architecture is a key element of bacterial cellular organization. Cell Microbiol 15:45–52. doi:10.1111/cmi.12049

Ptacin JL, Lee SF, Garner EC et al (2010) A spindle-like apparatus guides bacterial chromosome segregation. Nat Cell Biol 12:791–798. doi:10.1038/ncb2083

Rasnik I, McKinney SA, Ha T (2006) Nonblinking and long-lasting single-molecule fluorescence imaging. Nat Methods 3:891–893. doi:10.1038/nmeth934

Rieger B, Stallinga S (2013) The lateral and axial localization uncertainty in super-resolution light microscopy. ChemPhysChem. doi:10.1002/cphc.201300711

Rowland DJ, Biteen JS (2013) Top-hat and asymmetric gaussian-based fitting functions for quantifying directional single-molecule motion. ChemPhysChem. doi:10.1002/cphc.201300774

Rust MJ, Bates M, Zhuang X (2006) Sub-diffraction-limit imaging by stochastic optical reconstruction microscopy (STORM). Nat Methods 3:793–795. doi:10.1038/nmeth929

Santos A, Young IT (2000) Model-Based Resolution: applying the theory in quantitative microscopy. Appl Opt 39:2948–2958. doi:10.1364/AO.39.002948

Schoen I, Ries J, Klotzsch E et al (2011) Binding-activated localization microscopy of DNA structures. Nano Lett 11:4008–4011. doi:10.1021/nl2025954

Sengupta P, Jovanovic-Talisman T, Skoko D et al (2011) Probing protein heterogeneity in the plasma membrane using PALM and pair correlation analysis. Nat Methods 8:969–975. doi:10.1038/nmeth.1704

Shaner NC, Lin MZ, McKeown MR et al (2008) Improving the photostability of bright monomeric orange and red fluorescent proteins. Nat Methods 5:545–551. doi:10.1038/nmeth.1209

Sharonov A, Hochstrasser RM (2006) Wide-field subdiffraction imaging by accumulated binding of diffusing probes. Proc Natl Acad Sci USA 103:18911–18916. doi:10.1073/pnas.0609643104

Shtengel G, Galbraith JA, Galbraith CG et al (2009) Interferometric fluorescent super-resolution microscopy resolves 3D cellular ultrastructure. Proc Natl Acad Sci USA 106:3125–3130. doi:10.1073/pnas.0813131106

Steinhauer C, Forthmann C, Vogelsang J, Tinnefeld P (2008) Super-resolution microscopy on the basis of engineered dark states. J Am Chem Soc 130:16840–16841. doi:10.1021/ja806590m

Subach FV, Patterson GH, Manley S et al (2009) Photoactivatable mCherry for high-resolution two-color fluorescence microscopy. Nat Methods 6:153–159. doi:10.1038/nmeth.1298

Subach FV, Zhang L, Gadella TWJ et al (2010) Red fluorescent protein with reversibly photoswitchable absorbance for photochromic FRET. Chem Biol 17:745–755. doi:10.1016/j.chembiol.2010.05.022

Subach OM, Patterson GH, Ting L-M et al (2011) A photoswitchable orange-to-far-red fluorescent protein, PSmOrange. Nat Methods 8:771–777. doi:10.1038/nmeth.1664

Subach OM, Entenberg D, Condeelis JS, Verkhusha VV (2012) A FRET-facilitated photoswitching using an orange fluorescent protein with the fast photoconversion kinetics. J Am Chem Soc 134:14789–14799. doi:10.1021/ja3034137

Swoboda M, Henig J, Cheng H-M et al (2012) Enzymatic oxygen scavenging for photostability without pH drop in single-molecule experiments. ACS Nano 6:6364–6369. doi:10.1021/nn301895c

Szymborska A, de Marco A, Daigle N et al (2013) Nuclear pore scaffold structure analyzed by super-resolution microscopy and particle averaging. Science 341:655–658. doi:10.1126/science.1240672

Thompson RE, Larson DR, Webb WW (2002) Precise nanometer localization analysis for individual fluorescent probes. Biophys J 82:2775–2783

Thompson MA, Casolari JM, Badieirostami M et al (2010) Three-dimensional tracking of single mRNA particles in Saccharomyces cerevisiae using a double-helix point spread function. Proc Natl Acad Sci USA 107:17864–17871. doi:10.1073/pnas.1012868107

Tsien RY (1998) The green fluorescent protein. Annu Rev Biochem 67:509–544. doi:10.1146/annurev.biochem.67.1.509

Van de Linde S, Krstić I, Prisner T et al (2011a) Photoinduced formation of reversible dye radicals and their impact on super-resolution imaging. Photochem Photobiol Sci 10:499–506. doi:10.1039/c0pp00317d

Van de Linde S, Löschberger A, Klein T et al (2011b) Direct stochastic optical reconstruction microscopy with standard fluorescent probes. Nat Protoc 6:991–1009. doi:10.1038/nprot.2011.336

Vaughan JC, Dempsey GT, Sun E, Zhuang X (2013) Phosphine quenching of cyanine dyes as a versatile tool for fluorescence microscopy. J Am Chem Soc 135:1197–1200. doi:10.1021/ja3105279

Vogelsang J, Kasper R, Steinhauer C et al (2008) A reducing and oxidizing system minimizes photobleaching and blinking of fluorescent dyes. Angew Chem Int Ed Engl 47:5465–5469. doi:10.1002/anie.200801518

Vogelsang J, Cordes T, Forthmann C et al (2009) Controlling the fluorescence of ordinary oxazine dyes for single-molecule switching and superresolution microscopy. Proc Natl Acad Sci USA 106:8107–8112. doi:10.1073/pnas.0811875106

Wiedenmann J, Ivanchenko S, Oswald F et al (2004) EosFP, a fluorescent marker protein with UV-inducible green-to-red fluorescence conversion. Proc Natl Acad Sci USA 101:15905–15910. doi:10.1073/pnas.0403668101

Xu K, Zhong G, Zhuang X (2013) Actin, spectrin, and associated proteins form a periodic cytoskeletal structure in axons. Science 339:452–456. doi:10.1126/science.1232251